Metallic 1T phase source/drain electrodes for field effect transistors from chemical vapor deposited MoS2

Rajesh Kappera, Damien Voiry, Sibel Ebru Yalcin, Wesley Jen, Muharrem Acerce, Sol Torrel, Brittany Branch, Sidong Lei, Weibing Chen, Sina Najmaei, Jun Lou, Pulickel M. Ajayan, Gautam Gupta, Aditya D. Mohite, and Manish Chhowalla

Citation: APL Materials **2**, 092516 (2014); doi: 10.1063/1.4896077
View online: http://dx.doi.org/10.1063/1.4896077
View Table of Contents: http://scitation.aip.org/content/aip/journal/aplmater/2/9?ver=pdfcov
Published by the AIP Publishing

APL MATERIALS **2**, 092516 (2014)

Metallic 1T phase source/drain electrodes for field effect transistors from chemical vapor deposited MoS_2

Rajesh Kappera,[1] Damien Voiry,[1] Sibel Ebru Yalcin,[2] Wesley Jen,[1] Muharrem Acerce,[1] Sol Torrel,[1] Brittany Branch,[2] Sidong Lei,[3] Weibing Chen,[3] Sina Najmaei,[3] Jun Lou,[3] Pulickel M. Ajayan,[3] Gautam Gupta,[2] Aditya D. Mohite,[2] and Manish Chhowalla[1,a]

[1]*Materials Science and Engineering, Rutgers University, 607 Taylor Road, Piscataway, New Jersey 08854, USA*

[2]*MPA-11 Materials Synthesis and Integrated Devices, Los Alamos National Laboratory, Los Alamos, New Mexico 87545, USA*

[3]*Mechanical Engineering and Materials Science Department, Rice University, Houston, Texas 77005, USA*

(Received 15 July 2014; accepted 28 August 2014; published online 25 September 2014)

Two dimensional transition metal dichalcogenides (2D TMDs) offer promise as opto-electronic materials due to their direct band gap and reasonably good mobility values. However, most metals form high resistance contacts on semiconducting TMDs such as MoS_2. The large contact resistance limits the performance of devices. Unlike bulk materials, low contact resistance cannot be stably achieved in 2D materials by doping. Here we build on our previous work in which we demonstrated that it is possible to achieve low contact resistance electrodes by phase transformation. We show that similar to the previously demonstrated mechanically exfoliated samples, it is possible to decrease the contact resistance and enhance the FET performance by locally inducing and patterning the metallic 1T phase of MoS_2 on chemically vapor deposited material. The device properties are substantially improved with 1T phase source/drain electrodes. [http://dx.doi.org/10.1063/1.4896077]

Short channel effects in current state of the art electronics lead to substantial finite current in the off state, which in turn increases the standby power consumption. Heat dissipation is also a major concern in nanoscale electronics. The undesirable coupling of source/drain regions and the channel also increases with decreasing feature size. The latter can be attributed to poor electrostatics between the gate and the channel. Thus there is a substantial need to find new semiconductors that are compatible with existing complementary metal oxide semiconductor (CMOS) infrastructure and can mitigate the short channel effects. Recent progress in two dimensional (2D) materials suggests that such ultrathin materials could be one pathway towards future electronics. Substantial research has been devoted to graphene, the original 2D material, and although many interesting phenomena have been reported, the absence of a band gap makes it less desirable for implementation within the existing paradigm. Despite this, the knowledge gained over the past ten years in synthesis, processing, handling, device fabrication, and testing has been tremendously helpful in discovery of other 2D materials. In particular, monolayers of transition metal dichalcogenides (TMDs) with the generalized formula of MX_2, where M is a transition metal (from Groups 4 to 7 in the periodic table) and X is a chalcogen (S, Se, or Te), have received substantial interest.[1–4] Recent work on devices fabricated from TMDs such as MoS_2 and WSe_2 has revealed that they possess high mobility values, near theoretical subthreshold swing values, and interesting optical properties.[5–8]

[a]Author to whom correspondence should be addressed. Electronic mail: manish1@rci.rutgers.edu

Although the progress in TMDs has been rapid, key fundamental questions remain. For example, MoS_2 field effect transistors (FETs) are always n-type but the root cause of this behavior is unknown.[5,6] Controllable doping of 2D materials is problematic since implantation can severely damage the atomically thin materials and non-covalent functionalization to modulate conductivity can be chemically unstable. Fermi level pinning due to large concentration of carriers from sulfur vacancies has been suggested as a possible reason.[9–11] Local heterogeneity in structure,[12] chemistry,[13] and rhenium doping in natural minerals and precursors has also been observed. Substantial effort is also being devoted to large-scale synthesis of uniform monolayered TMDs by chemical vapor deposition.[14–17] In addition to materials related issues, large contact resistance values ranging from 0.7 kΩ μm to 1.5 kΩ μm have been reported[18–20] leading to Schottky type behavior. To understand the role of contacts, researchers have investigated a variety of metals on thin MoS_2.[9,21] Low work function metals such as scandium were found to yield the lowest contact resistance values.[9]

Very recently, we have demonstrated that it is possible to utilize the metallic 1T phase of MoS_2 as the source and drain electrodes in FETs in which the channel is mechanically exfoliated ultra-thin 2H phase MoS_2.[22] Devices fabricated using the 1T phase as the electrodes exhibited consistently superior performance to those with metal electrodes deposited directly on top of the semiconducting 2H phase. We attribute the superior performance of the devices to absence of structural and electrical mismatch. In this contribution, we extend this work to purely single layer chemical vapor deposited MoS_2 samples and show that the device characteristics are comparable to those of the mechanically exfoliated samples.

It is well known that TMDs can exist in several different structural phases. For example, the 1T phase is thermodynamically stable in complex metals such as TaS_2. In contrast, the 2H phase is thermodynamically stable in semiconducting TMDs such as MoS_2. It has been known for sometime that it is possible to induce the 1T phase in semiconducting TMDs. The original work by Frindt and co-workers on chemical exfoliation of MoS_2 using lithium intercalation revealed the presence of the 1T phase in the monolayered flakes.[23,24] After this work, Kanatzidis and his group reported substantial work on synthesis and characterization of monolayered nanosheets of TMDs containing different phases.[25] The metastable 1T phase is induced by charge transfer from the organic component of the lithium compound (typically butyl lithium). To accommodate this additional charge, the 2H phase undergoes a phase transformation to the metallic 1T phase. However, the large amount of additional charge on the MoS_2 must be balanced by counter ions. This is typically not a problem for exfoliated nanosheets in solution since there are numerous counter ions present to balance the charge. However, we have also shown that once induced, the 1T phase can also be stabilized in "dry" thin films.[26–28] In the thin films, the charge is likely to be balanced either by protons or other positive ions, most likely from adsorbed water. We have confirmed that impurities such as Li ions are not present in the 1T phase.[29,30] Once induced, the 1T phase is reasonably stable with activation energy of approximately 1 eV needed for relaxation.[29,31,32] Furthermore, full relaxation of 2H phase can be induced by annealing the 1T phase in vacuum or controlled atmosphere. Thus, it is possible to engineer the phases in semiconducting TMDs by chemistry to convert the 2H phase to metallic 1T phase and by annealing to convert the metastable 1T phase to the stable 2H phase.

In this paper, we describe the synthesis of high quality, uniform, and triangular 2H phase monolayered MoS_2 nanosheets with dimensions of tens of micrometers. We have optimized the FET properties from such CVD nanosheets by implementing the 1T phase as the source and drain electrodes. The contact resistance in the devices was found to be $\sim$200 Ω μm, consistent with our previous results.[22] We show that the 1T electrodes dramatically improve the device performance with mobility values of 56 cm^2/V s, exceptionally large on state currents of 110 μA/μm, and subthreshold swing values of 0.72 V/decade. All of these values are substantially better than metal electrodes deposited directly on top of the 2H phase.

Silicon substrates capped with 285 nm of oxide were used for MoS_2 growth. The substrates were placed on top of an alumina crucible containing 20 mg of MoO_3 (Sigma-Aldrich) at the center of the furnace. One hundred milligrams of sulfur powder (Sigma-Aldrich) in a separate crucible was placed in the cooler part of the furnace near the gas inlet. The growth was performed at 750 °C for 15 min at 1 atm of 95% argon and 5% hydrogen. Typical optical and atomic force microscopy images of CVD grown triangular MoS_2 monolayers are shown in Figures 1(a) and 1(b), respectively.

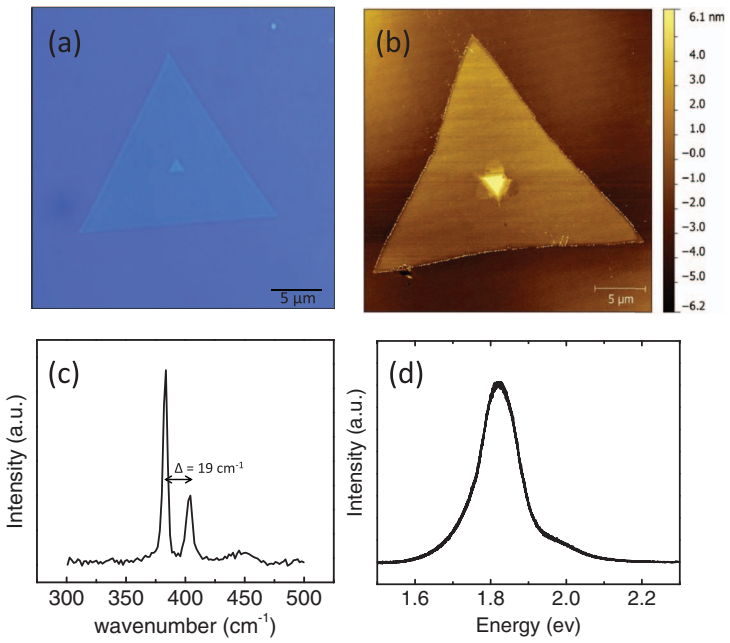

FIG. 1. (a) Optical microscopy image of a typical triangle grown by chemical vapor deposition on SiO_2. (b) The corresponding AFM image. The nucleation site can be seen in the center of the triangle. (c) Raman spectrum of the CVD grown material. The two peaks correspond to the 2H phase of bulk MoS_2. (d) Typical PL spectrum of the CVD grown material. The main A and B exciton peaks are visible.

The thickness obtained from AFM analyses was found to be ∼0.8 nm, consistent with that of a monolayer. Thicker nucleation seed at the center of the triangular sheet can also be observed. A representative Raman spectrum of the monolayer MoS_2 is shown in Figure 1(c). The Raman E^1_{2g} and A_{1g} modes near 400 cm^{-1} of the bulk MoS_2 can be clearly seen in the single layer.[24] In particular, the CVD samples show a strong in-plane vibrational mode at ∼384 cm^{-1} corresponding to the E^1_{2g} mode of the bulk 2H-MoS_2 crystal. A representative photoluminescence (PL) spectrum of the CVD MoS_2 is shown in Figure 2(d). The pronounced PL peak at ∼1.8 eV along with a small shoulder peak at ∼1.9 eV can be attributed to the A and B excitons in single layered MoS_2. The A and B excitons arise from direct band transitions at the K-point in the Brillouin zone. These results suggest that the CVD grown material is single layer MoS_2 that is semiconducting (i.e., the 2H phase) with reasonable good structural integrity.

The structural conversion from the semiconducting 2H phase to the metallic 1T phase using butyl lithium is shown in Figure 2. To perform the phase transformation, samples were immersed into 5 ml of 1.6M n-butyl lithium (Sigma-Aldrich) for 48 hours. All the butyl lithium exposure was done in the glove box in argon atmosphere at room temperature. Using simple lithography to create well ordered masks, we locally patterned the 1T phase as shown in Figures 2(a) and 2(b). That is, by exposing regions to butyl lithium, it is possible to convert them to 1T phase while masked regions remain as the 2H phase. The dark strips in Figures 2(a) and 2(b) represent the regions exposed to the butyl lithium and therefore converted to the metallic 1T phase. The conversion was confirmed by performing PL mapping as shown in Figure 2(a) where pronounced bright PL can be observed from the 2H region and no PL is observed from the 1T phase region. The PL spectra of the 1T and 2H phases are shown in Figure 2(c). The PL is completely quenched in the 1T phase due to its metallic nature while the PL in the 2H phase remains unchanged after the butyl lithium chemical treatment. The Raman spectra of the 1T and 2H phases are shown in Figure 2(d). Additional new peaks consistent with the 1T phase are observed in the butyl lithium treated sample while the untreated regions show the features of the 2H phase. We have confirmed the concentration of the 1T phase using x-ray photoelectron spectroscopy (XPS, not shown) and found it to be ∼70%. These results clearly demonstrate that it is possible to locally induce a phase change in CVD grown MoS_2.

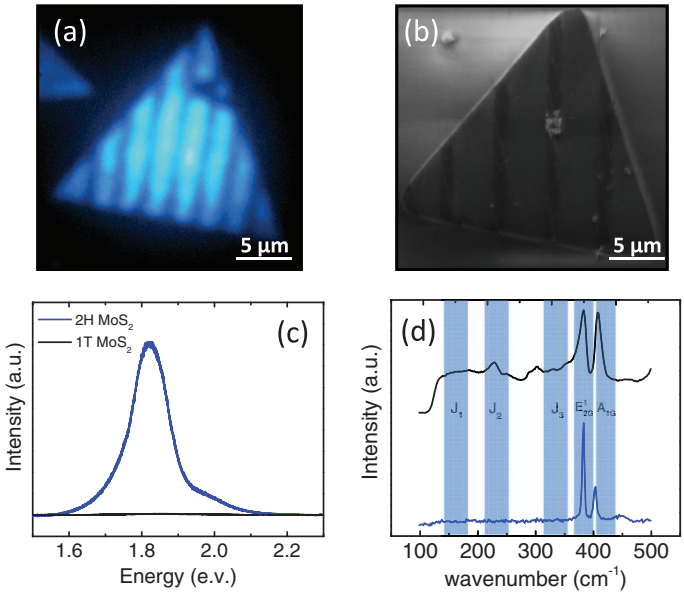

FIG. 2. (a) PL map of a CVD grown nanosheet patterned with 1T phase strips. The dark strips represent the 1T phase where the PL has been quenched. The bright regions indicate that the 2H phase is unaffected by the chemical treatment. (b) SEM image shows different contrast between the 1T and 2H phases. (c) PL spectra of the 1T and 2H phases. The PL is completely quenched in the metallic 1T phase. (d) Raman spectra of the 1T phase (top) and the 2H phase. New peaks can be observed in the 1T phase spectrum.

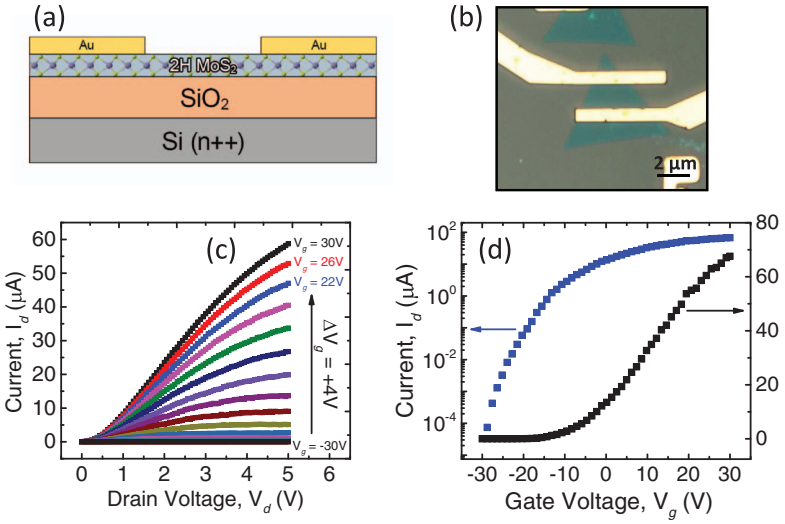

FIG. 3. (a) Device schematic of a bottom gated FET with Au deposited directly on the 2H phase MoS_2. (b) Optical microscopy image of the devices. (c) Output and (d) transfer characteristics of the device.

We have fabricated bottom gated FETs using CVD grown MoS_2. Two types of source and drain electrode configurations in FETs were tested: one in which the gold electrodes were deposited directly on top of the 2H phase and the other in which the Au electrodes were deposited on 1T phase. In both cases, the channel was the semiconducting 2H phase. The schematic of the former device configuration (Au directly on 2H phase) is shown in Figure 3(a). The optical microscopy photograph of the device is shown in Figure 3(b). The output and transfer characteristics of the FET are shown in Figures 3(c) and 3(d), respectively. The devices exhibit good saturation and high on state currents. The mobility values extracted from the measurements are ~25 cm^2/V s.

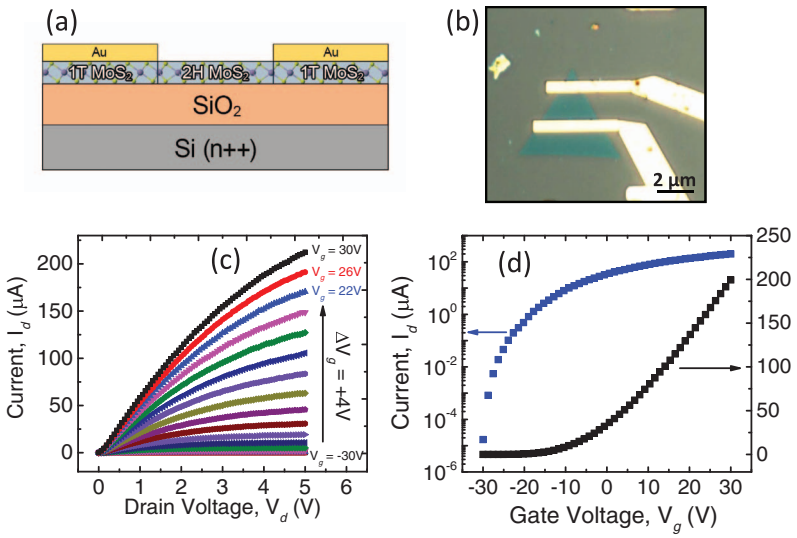

FIG. 4. (a) Device schematic of a bottom gated FET with Au deposited on the patterned 1T phase MoS_2. (b) Optical microscopy image of the devices. (c) Output and (d) transfer characteristics of the device.

TABLE I. Comparison of the device properties of FETs with 2H phase and 1T phase electrodes.

Property	2H phase contacts	1T phase contacts
ON current (μA/μm)	4.2	110
Transconductance (μS/μm)	2.2	4.8
Mobility (cm^2/V s)	24	56
Subthreshold swing (V/decade)	1.59	0.72

Device schematic of FETs with 1T phase source/drain electrodes and 2H phase channel is shown in Figure 4(a). The optical microscopy photograph of the device is shown in Figure 4(b). The output and transfer characteristics of the FETs are shown in Figures 4(c) and 4(d), respectively. The mobility of the 1T phase electrode devices was found to be ~55 cm^2/V s. The saturation behavior in the 1T phase electrode devices is better than in the case of Au on 2H phase devices. The on state current is also substantially larger. The comparison of key values from the two types of devices is provided in Table I. It can be seen that the on state current, transconductance, mobility, and subthreshold swing values are substantially better in the 1T phase contacts. These results suggest that charge injection into the channel is more efficient with 1T contacts. The lower subthreshold swing values in the 1T phase electrode devices could be due to lower density of interface traps. We also found that during conversion, some butyl lithium diffuses into the masked channel, which leads to conversion from 2H to 1T. Thus the effective channel length is shorter than expected. In addition, the 1T contacts are side contacts, which have been shown to be more effective than vertical contacts.[6,9]

In conclusion, we have demonstrated that it is possible to locally convert and pattern the metastable metallic 1T phase in MoS_2 using chemistry. We show that the metallic 1T phase contacts are effective electrodes for high performance FETs from CVD grown MoS_2 monolayers. The device characteristics with the 1T phase demonstrate higher on state currents, mobilities, and better subthreshold swing values.

[1] L. F. Mattheiss, Phys. Rev. B **8**, 3719 (1973).
[2] J. A. Wilson and A. D. Yoffe, Adv. Phys. **18**, 193 (1969).
[3] A. D. Yoffe, "Layer compounds," Annu. Rev. Mater. Sci. **3**, 147 (1973).
[4] A. D. Yoffe, Adv. Phys. **42**, 173 (1993).
[5] B. Radisavljevic, A. Radenovic, J. Brivio, V. Giacometti, and A. Kis, Nat. Nanotechnol. **6**, 147 (2011).
[6] S. Kim, A. Konar, W. S. Hwang, J. H. Lee, J. Lee, J. Yang, C. Jung, H. Kim, J. B. Yoo, J. Y. Cho, Y. W. Jin, S. Y. Lee, D. Jena, W. Choi, and K. Kim, Nat. Commun. **3**, 1011 (2012).

[7] W. Liu, J. Kang, D. Sarkar, Y. Khatami, D. Jena, and K. Banerjee, Nano Lett. **13**, 1983 (2013).
[8] H. Fang, S. Chuang, T. C. Chang, K. Takei, T. Takahashi, and A. Javey, Nano Lett. **12**, 3788 (2012).
[9] S. Das, H. Y. Chen, A. V. Penumatcha, and J. Appenzeller, Nano Lett. **13**, 100 (2013).
[10] C. Gong, L. Colombo, R. M. Wallace, and K. Cho, Nano Lett. **14**, 1714 (2014).
[11] S. McDonnell, R. Addou, C. Buie, R. M. Wallace, and C. L. Hinkle, ACS Nano **8**, 2880 (2014).
[12] W. Zhou, X. Zou, S. Najmaei, Z. Liu, Y. Shi, J. Kong, J. Lou, P. M. Ajayan, B. I. Yakobson, and J. C. Idrobo, Nano Lett. **13**, 2615 (2013).
[13] S. Najmaei, X. Zou, D. Er, J. Li, Z. Jin, W. Gao, Q. Zhang, S. Park, L. Ge, S. Lei, J. Kono, V. B. Shenoy, B. I. Yakobson, A. George, P. M. Ajayan, and J. Lou, Nano Lett. **14**, 1354 (2014).
[14] Y. H. Lee, X. Q. Zhang, W. Zhang, M. T. Chang, C. T. Lin, K. D. Chang, Y. C. Yu, J. T. W. Wang, C. S. Chang, L. J. Li, and T. W. Lin, Adv. Mater. **24**, 2320 (2012).
[15] A. M. van der Zande, P. Y. Huang, D. A. Chenet, T. C. Berkelbach, Y. You, G. H. Lee, T. F. Heinz, D. R. Reichman, D. Muller, and J. C. Hone, Nat. Mater. **12**, 554 (2013).
[16] S. Najmaei, Z. Liu, W. Zhou, X. Zou, G. Shi, S. Lei, B. I. Yakobson, J. C. Idrobo, P. M. Ajayan, and J. Lou, Nat. Mater. **12**, 754 (2013).
[17] W. Wu, D. De, S. C. Chang, Y. Wang, H. Peng, J. Bao, and S. S. Pei, Appl. Phys. Lett. **102**, 142106 (2013).
[18] S. Das and J. Appenzeller, Nano Lett. **13**, 3396 (2013).
[19] H. Liu, A. T. Neal, and P. D. Ye, ACS Nano **6**, 8563 (2012).
[20] H. Liu, M. Si, Y. Deng, A. T. Neal, Y. Du, S. Najmaei, P. M. Ajayan, J. Lou, and P. D. Ye, ACS Nano **8**, 1031 (2014).
[21] C. Gong, C. Huang, J. Miller, L. Cheng, Y. Hao, D. Cobden, J. Kim, R. S. Ruoff, R. M. Wallace, K. Cho, X. Xu, and Y. J. Chabal, ACS Nano **7**, 11350 (2013).
[22] R. Kappera, D. Voiry, S. E. Yalcin, B. Branch, G. Gupta, A. D. Mohite, and M. Chhowalla, "Phase-engineered low-resistance contacts for ultra-thin MoS_2 transistors," Nat. Mater. (2014).
[23] P. Joensen, R. F. Frindt, and S. R. Morrison, Mater. Res. Bull. **21**, 457 (1986).
[24] S. Jiménez Sandoval, D. Yang, R. F. Frindt, and J. Irwin, Phys. Rev. B **44**, 3955 (1991).
[25] J. Heising and M. G. Kanatzidis, J. Am. Chem. Soc. **121**, 638 (1999).
[26] G. Eda, H. Yamaguchi, D. Voiry, T. Fujita, M. Chen, and M. Chhowalla, Nano Lett. **11**, 5111 (2011).
[27] G. Eda, T. Fujita, H. Yamaguchi, D. Voiry, M. Chen, and M. Chhowalla, ACS Nano **6**, 7311 (2012).
[28] D. Voiry, M. Salehi, R. Silva, T. Fujita, M. Chen, T. Asefa, V. B. Shenoy, G. Eda, and M. Chhowalla, Nano Lett. **13**, 6222 (2013).
[29] D. Voiry, H. Yamaguchi, J. Li, R. Silva, D. C. B. Alves, T. Fujita, M. Chen, T. Asefa, V. B. Shenoy, G. Eda, and M. Chhowalla, Nat. Mater. **12**, 850 (2013).
[30] M. Chhowalla, H. S. Shin, G. Eda, L.-J. Li, K. P. Loh, and H. Zhang, Nat. Chem. **5**, 263 (2013).
[31] F. Wypych and R. Schillhorn, J. Chem. Soc. Chem. Commun. **1992**, 1386.
[32] H.-L. Tsai, J. Heising, J. L. Schindler, C. R. Kannewurf, and M. G. Kanatzidis, Chem. Mater. **9**, 879 (1997).